Title

Non-targeting siRNA induces NPGPx expression to cooperate with exoribonuclease XRN2 for releasing the stress

Journal

Nucleic Acids Research, 40(1)

ISSN

0305-1048 1362-4962

Authors

Wei, P.-C.
Lo, W.-T.
Su, M.-I.
et al.

Publication Date

2011-09-09

DOI

10.1093/nar/gkr714

Published online 9 September 2011

Nucleic Acids Research, 2012, Vol. 40, No. 1 ***323–332***
doi:10.1093/nar/gkr714

Non-targeting siRNA induces NPGPx expression to cooperate with exoribonuclease XRN2 for releasing the stress

Pei-Chi Wei[1,2], Wen-Ting Lo[2,3], Mei-I. Su[3], Jin-Yuh Shew[1,2,*] and Wen-Hwa Lee[2,4,*]

[1]Graduate Institute of Life Sciences, National Defense Medical Center, [2]Genomics Research Center, Academia Sinica, [3]Institute of Biological Chemistry, Academia Sinica, Taipei, Taiwan and [4]Department of Biological Chemistry, University of California, Irvine, CA 92697-4037, USA

Received March 9, 2011; Revised August 12, 2011; Accepted August 18, 2011

ABSTRACT

Short interfering RNAs (siRNAs) target specific mRNAs for their degradation mediated by RNA-induced silencing complex (RISC). Persistent activation of siRNA-RISC frequently leads to non-targeting toxicity. However, how cells mediate this stress remains elusive. In this communication, we found that the presence of non-targeting siRNA selectively induced the expression of an endoplasmic reticulum (ER)-resident protein, non-selenocysteine containing phospholipid hydroperoxide glutathione peroxidase (NPGPx), but not other ER-stress proteins including GRP78, Calnexin and XBP1. Cells suffering from constant non-targeting siRNA stress grew slower and prolonged G1 phase, while NPGPx-depleted cells accumulated mature non-targeting siRNA and underwent apoptosis. Upon the stress, NPGPx covalently bound to exoribonuclease XRN2, facilitating XRN2 to remove accumulated non-targeting siRNA. These results suggest that NPGPx serves as a novel responder to non-targeting siRNA-induced stress in facilitating XRN2 to release the non-targeting siRNA accumulation.

INTRODUCTION

RNA induced post-transcriptional gene silencing (PTGS) is one of the important regulation mechanisms in biological processes. PTGS, also known as RNA interference (RNAi), was first observed in plants and *Caenorhabditis elegans* (1,2). In *C. elegans*, it was found that genes could be silenced by sequence-specific double-stranded (ds)RNA (3). The long dsRNA was processed into 22-nt short interfering dsRNA (siRNA) (4), unwound (5) and then loaded on its mRNA targets to promote their degradation via antisense pairing (6). Gene silencing can be triggered by exogenous dsRNAs and endogenous non-coding hairpin-structured RNAs, such as microRNAs (miRNAs). To date, over 700 miRNAs have been discovered. miRNAs mediate gene silencing through retardation of mRNA translation or, similar to siRNAs, through degradation of mRNA (7). Both siRNAs and miRNAs have been shown to be important in regulating gene expression and participate in many biological processes including development, differentiation, cell growth and death.

RISC has a critical role in the process of gene silencing (4–6). siRNA or miRNA associated with RISC to form a siRISC complex and guides the complex to mRNA with complementary sequences. Once siRISC binds to the recognized mRNA, it activates RNase to cleave the target. However, accumulation of siRISC by either excess siRNAs or miRNAs may have deleterious effects to cells such as undesired off-targeting gene silencing or exhaustion of RISC. For example, excess siRNA against ICAM-1 leads to TNFR-1 mRNA degradation (8). Transfection of siRNAs against PPIB-1 resulted in off-targeting silencing of 347 genes, a process that was later identified to be dependent on the complementary of merely 7 nt between the siRNA and silenced genes (9). Also, off-targeting siRNA can lead to exhaustion of RISC that generates cellular stress and leads to cell growth retardation (10). SiRNA stress must be released to maintain normal cellular function. However, how cells mediate siRNA stress remains unclear.

Serendipitously, we found that expression of NPGPx, an endoplasmic reticulum (ER)-resident protein, was upregulated in cells when non-targeting siRNAs were introduced. These non-targeting siRNAs specifically induced NPGPx expression, but not other canonical

*To whom correspondence should be addressed. Tel: +886 2 2789 1255; Fax: +886 2 2789 8777; Email: jyshew@gate.sinica.edu.tw
Correspondence may also be addressed to Wen-Hwa Lee. Tel: +949 824 4492; Email: whlee@uci.edu

ER-stress responding genes. Cells under a constant non-targeting siRNA stress grew slower, while cells deficient of NPGPx accumulated non-targeting siRNA and underwent apoptosis. NPGPx bound to and colocalized with exoribonuclease XRN2 and was essential for the nuclease to remove the accumulated non-targeting siRNA. These results provided, in part, a potential mechanism to explain how cells resolve non-targeting siRNA stress.

MATERIAL AND METHODS

Lentivirus production and infection

pLKO-puro-shRNA vectors and empty vector pLKO-AS1 (referred to shEmpty) were purchased from National RNAi Core Facility (NRCF), Taiwan. Lentivirus packaging was performed followed by the manufacturer's instruction. In brief, 293T cells were grown to 80% confluence and transfected with pMD.G, pCMV-deltaR8.91 and pLKO-puro-shRNA using Lipofetamin 2000 (Invitrogen). The culture medium containing lentivirus was collected at 48 and 72 h after transfection. For infection, cells were grown to 70% confluence and infected with lentivirus (multiplicity of infection = 1) twice (6 h each) in culture medium supplemented with 8 μg/ml polybrene (Sigma H9268). Cells were selected using 2 μg/ml puromycin for 4 days.

RNAi transfection

Cells were transfected with indicated amount of RNAi against human NPGPx (Stealth RNAi, clone HSS142294, Invitrogen), mouse NPGPx, (Stealth RNAi, MSS250292, MSS250294), mouse XRN2 (Stealth RNAi, MSS280622), human PPIB-1 (Customized by Invitrogen. Forward: 5′-UUUgUAgCCAAAUCCUUUCUCUCCU-3′; reverse: 5′-AggAgAgAAAggAUUUggCUACAAA-3′) or control siRNA (Stealth RNAi, 12935-300, Invitrogen) using Lipofectamin 2000TM (Invitrogen). The control siRNA does not target to any gene in human, mouse or rat by screening with the NCBI RefSeq as provided by the manufacturer.

Plasmid construction

Human NPGPx was cloned in pLKO-AS2-Hygro vector with NheI and AscI restriction enzymes. XRN2 expression vector was received from Dr James Manley (Department of Biological Science, Columbia University).

Western blot analysis

Cells were lysed with RIPA buffer [50 mM Tris–HCl, pH = 7.4, 150 mM NaCl, 2 mM EDTA, 50 mM NaF, 1% Nonidet P-40, 0.5% sodium deoxycholate, 0.1% SDS and 1 mM phenylmethylsulfonyl fluoride and 1 mM dithiothreitol (DTT)], and clarified by centrifugation as described (11). Cell lysate was denatured in SDS sample buffer (50 mM DTT, 1% SDS, 50 mM Tris–HCl, pH = 6.8, 10% glycerol and 0.01% bromophenoblue), boiled at 95°C for 10 min and then subjected to sodium dodecyl sulfate polyacrylamide gel electrophoresis (SDS–PAGE) and western blot analysis. Primary antibodies against NPGPx (GeneTex, GTX70266), eIF2α (GeneTex, GTX25369), phosphorylated eIF2α (GeneTex, GTX30727), GRP78 (BD, 610978), Calnexin (Pierce, MA3-027), p53 (CalBiochem, OP-03), XNR2 (ab72181, Abcam) and α-tubulin (GeneTex, GTX11302) were used according to the manufacturers' instruction.

Immunoprecipitation assay

Cell lysates were collected from shLuc-transduced cells using Lysis-250 and precleaned with protein A/G agarose beads (11). NPGPx or XRN2 was precipitated from the clarified lysates with 1 μg antibodies against NPGPx (GTX108578, GeneTex) or XRN2 (ab72181, Abcam) as previous described (11). The precipitated protein complexes were separated by 8–16% gradient SDS–PAGE followed by western blot analysis.

Northern blot analysis

Total RNA was extracted from mouse embryonic fibroblasts (MEFs) transduced with shLuc using Trizol reagent (Invitrogen). Equal amount of total RNA from WT or NPGPx$^{-/-}$ MEFs (30 μg/lane) were separated in 15% TBE-UREA acrylamide PAGE (Novex® TBE-UREA Gels, Invitrogen). RNAs were transferred to Hybond™-N+ membrane (GE Healthcare), cross-linked by UV irradiation and following the hybridization procedures as previously described (12). Membranes were washed, and the siLuc signals were detected by LightShift assay (Thermo).

RNA extraction, reverse transcription, and PCR and quantitative real-time PCR analysis

Total RNA was extracted from cells using Trizol reagent (Invitrogen) and converted into cDNA by reverse transcription followed by the manufacture's instruction (ABI, 4368814). Specific cDNA amounts of following genes were determined using Syber Green-based RT–qPCR systems. Primers for human NPGPx (forward 5′-GCAGGAGCAGGACTTCTACGACTTC-3′ and reverse 5′-ACCGGTGACTGCAATCTTGCTAAAC-3′), human PPIB-1 (forward 5′-CCTCTTCCGGCCTCAGC TGTCCG-3′ and reverse 5′-CATGTTGCGTTCGGAG AGGCGC-3′) and human XBP-1 (forward 5′-TTGCTG AAGAGGAGGCGGAA3-′ and reverse 5′-ACAGAGAA AGGGAGGCTGGT-3′) were used. House-keeping genes such as S26 or β-actin served as internal controls (S26 primers: forward 5′-CCGTGCCTCCAAGATGAC AAAG-3′ and reverse 5′-ACTCAGCTCCTTACATGG GCTT-3′).

siRNA reverse transcription and qPCR analysis

Total RNA was extracted from cells for generating cDNA fragments of shLuc and siLuc using NCodeTM miRNA First-Strand cDNA Synthesis kit (MIRC-50) (Invitrogen). The quantities of shLuc and siLuc RNA were measured by quantitative real-time PCR (qPCR) using a primer covered the stem–loop region of shLuc (primer for shLuc, 5′-CTCGCTCGAGCGAGGGCGAC-3′) and

another primer covered the entire siLuc sequence (primer for siLuc, 5′-CCTAAGGTTAAGTCGCCCTCG-3′), respectively. U6 expression level was also determined for serving as an internal control (primer for U6, 5′-CGCA AGGATGACCAGCAAATTC-3′). qPCR was performed using MIRC-50 kit followed by the manufacture's instruction (Invitrogen).

Recombinant protein expression and purification

pET-48b vector, which contains thioredoxin and His as a tag (Novagen), was chosen for expressing NPGPx recombinant proteins to resolve the solubility issue in bacteria. pET-48b-NPGPx was constructed by inserting an BamHI and HindIII digested DNA fragment containing human NPGPx with TEV protease cutting site at its N-terminus into pET-48b. pET-48b-C2AS-NPGPx was generated by PCR-directed mutagenesis method to change Cys57 and Cys86 from the WT plasmid, pET-48b-NPGPx, into alanine (GCC) and serine (TCC). pET-15b-hXRN2 was constructed using pET-15b, which contains N-terminal his-tag followed with a TEV cutting site, to express XRN2 by ligand-independent cloning (LIC) method (13). pET-48b-NPGPx and pET-48b-C2AS-NPGPx were transformed into bacteria of BL21 (DE3), while pET-15b-hXRN2 was transformed into BL21 star. These his-tagged proteins were first purified by nickel beads (Sigma) and then digested with TEV protease to release tags, which was removed by rebinding to nickel beads. Finally, the desired proteins were further purified by gel filtration and the corresponding fractions were concentrated using Amicon Ultra-10 (Millipore).

To perform the *in vitro* binding assay, the purified NPGPx was treated with H_2O_2 first and incubated with nickel beads bound XRN2 for 20 min. The beads were then washed with 8 M Urea and the bound proteins were analyzed by western blot.

MEF preparation

The 13.5d NPGPx$^{+/+}$ and NPGPx$^{-/-}$ embryos (manuscript in preparation) were used for MEF preparation as previously described (14). In brief, embryos were washed with PBS, and chopped into small pieces in 1× trypsin. Processed embryos were incubated with trypsin at 37°C for 30 min, then stopped the digestion with 10% fetal bovine serum-containing low glucose dulbecco's modified eagle medium (DMEM). Cells were plated and cultured following the 3T3 culture protocol in which 10^6 cells were passed into a 10-cm dish every 3 days.

Immunofluorescence staining, Annexin V and γH2Ax staining

MEFs were washed with PBS, pre-extracted with buffer containing 80 mM PIPES, pH 7.0, 100 nM NaCl, 30% glycerol, 0.5% Triton X-100 for 5 min on ice and fixed with 4% paraformaldehyde [in phosphate buffer saline with Tween 20 (PBST) with 0.3% Triton X-100] at room temperature. The fixed cells were incubated with primary antibody against NPGPx (mouse polyclonal) and XRN2 (ab72181, Abcam) followed by corresponding secondary antibodies conjugated with florescence (For NPGPx: mouse IgG-FITC; XRN2: rabbit IgG-PE) and then visualized by florescence microscopy. For apoptotic cell detection, MEFs were costained with Annexin V (Molecular Probes, A13201) and propidium iodide (Sigma, P4170) and analyzed by FACS analysis. For γH2Ax staining, MEFs transduced with shLuc or control vector (shEmpty) were fixed with 4% paraformaldehyde, permeablized with 0.2% Tween-20 (in PBST), and subsequently stained with anti-γH2Ax antibody (Novus, NB100-384). 4′,6-diamidino-2-phenylindole (DAPI) was used for DNA staining. The stained cells were visualized by confocal microscopy.

Cell growth assay

Different passages of NPGPx$^{+/+}$ or NPGPx$^{-/-}$ MEFs transduced with viruses either containing shRNA or NPGPx cDNA were seeded in 60 mm culture dishes (1×10^5 cells per dish) with puromycin-containing low-glucose DMEM and incubated in humidified CO_2 incubator (37°C, 5% CO_2). Medium was changed every 2 days and cell number was counted every 24 h. For late phase cell growth assay, MEFs were transduced with shLuc at passage 1 and then kept in culture for another 4 passages. Cells were seeded in 60 mm culture dishes at passage 5 and cell numbers were counted every 24 h, respectively.

RESULTS

Non-targeting shRNA/siRNA induces NPGPx expression

In viral shRNA delivery systems, shRNA against non-mammalian genes such as luciferase (shLuc), red fluorescent protein (shRFP) or LacZ (shLacZ) are commonly employed as a control for most of the RNA knockdown experiments. Using these control shRNAs, we surprisingly found that NPGPx expression was increased about 3-fold compared with the cells infected with the virus carrying no shRNA (Figure 1a and b) and that upregulation prolonged about a month in culture. To confirm NPGPx induction resulted from the expressed non-targeting siRNA, we then used chemically synthesized control siRNA, which did not match with any transcripts of human, mouse or rat for transfection (Invitrogen). NPGPx induction was observed in a dose-dependent manner in cells transfected with increasing amount of non-targeting siRNA (Figure 1c). Moreover, not only the protein, the NPGPx mRNA was also upregulated in the non-targeting shRNA expressing cells compared with the control (Figure 1d). When transfecting with a known off-targeting siRNA, PPIB-1 (9), the expression of NPGPx was not increased (Figure 1e and f), suggesting that the induction of NPGPx expression was not from off-targeting siRNA. Thus, it is likely that the upregulation of NPGPx may result from siRNA that has no cognate target. To test this possibility, we expressed Luciferase mRNA in cells containing shLuc and found that the NPGPx expression was diminished (Figure 1g). Because NPGPx primarily resides in ER (see below), we then tested whether ER stress response could be triggered by the non-targeting shRNA/siRNA.

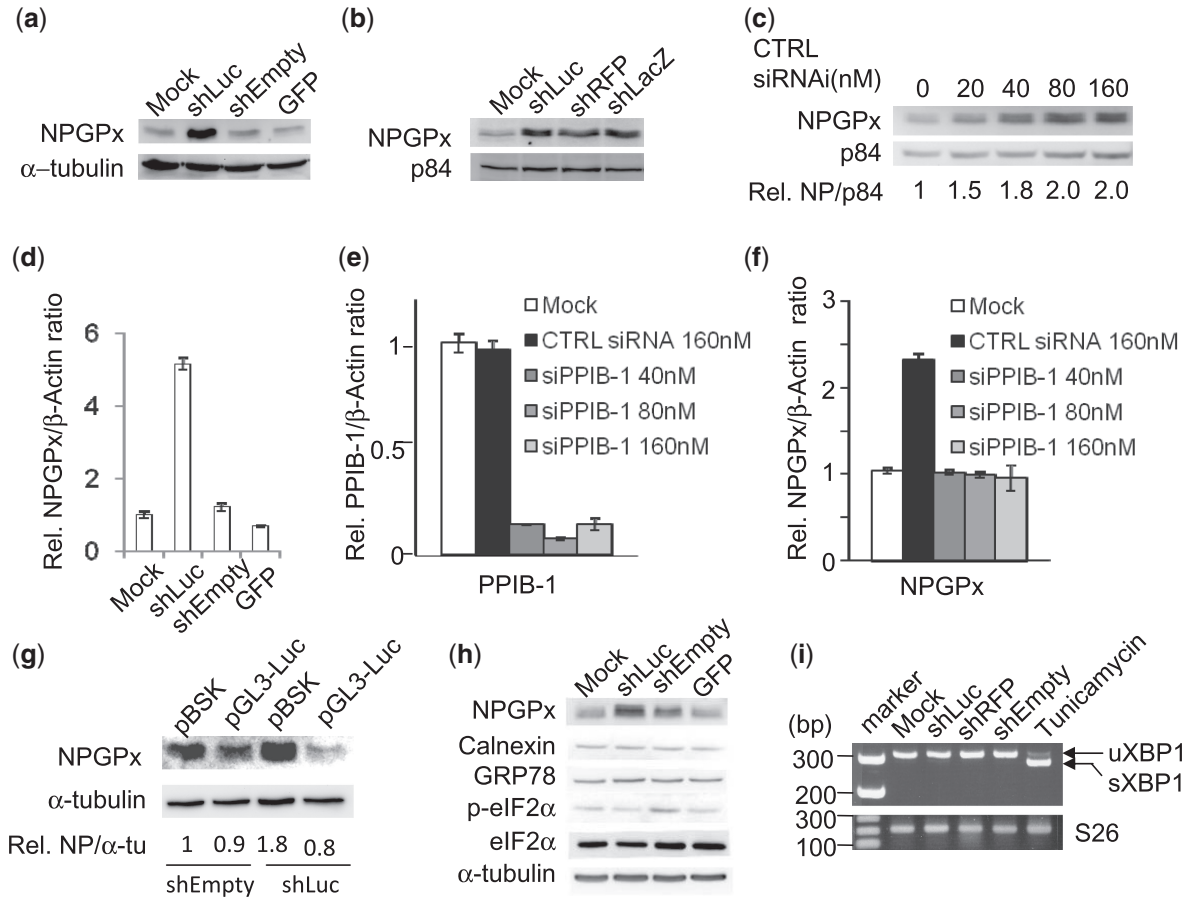

Figure 1. NPGPx expression was induced by non-targeting shRNA/RNAi. (**a** and **b**) Western blot analysis of NPGPx, p84 and α-tubulin proteins from WI38 cells infected with lentivirus carrying shLuc, shRFP, shLacZ, GFP, shEmpty (shRNA cloning vector) or uninfected as control. Specific antibodies against each protein were used as probes. p84 and α-tubulin served as internal loading controls. (**c**) Western blot analysis of NPGPx protein level in WI38 cells transfected with various amount of non-targeting siRNA (CTRL siRNA). Relative NPGPx/p84 ratio was shown in below. (**d**) NPGPx mRNA expression analyzed by RT–qPCR from WI38 cells infected with lentivirus carrying with shLuc, GFP or control vector (shEmpty) or uninfected as control (mock). Relative NPGPx mRNA level (normalized with β-actin and compare with Mock) was shown. (**e** and **f**) RT–qPCR analysis. WI38 cells transfected with non-targeting siRNA (Ctrl siRNA, 160 nM) or PPIB-1 siRNA were used in this assay. The PPIB-1 mRNA amount (e) and NPGPx mRNA expression level (f) were shown. Mock: WI38 cells without siRNA transfection. (**g**) Western blot analysis of WI38 cells infected with vector control (shEmpty) or shLuc, and then transfected with either pBSK or Luciferase expression vector (pGL3-Luc). Cell lysates were harvested 48 h after transfection for western blot analysis. Relative expression ratio of NPGPx/α-tubulin (Rel. NP/α-tu) was calculated. (**h**) Expressions of stress-related proteins including NPGPx, Calnexin, GRP78, eIF2α, phospho-eIF2α (p-eIF2α) in WI38 cells infected with lentivirus carrying shLuc, GFP, shRNA cloning vector (shEmpty) or uninfected as control (mock). α-Tubulin served as an internal loading control. (**i**) Expression of unspliced (uXBP1) or spliced (sXBP1) XBP1 mRNA analyzed by RT–PCR from WI38 cells infected with lentivirus carrying with shLuc, shRFP, shEmpty or uninfected as the control (mock). Cells treated with tunicamycin (2 μg/ml for 8 h) served as a positive control, where spliced XBP1 (sXBP1) was detected. Ribosomal RNA S26 served as an internal loading control. Each experiment has been repeated at least twice, and the representative data from one of these experiments were shown.

As shown in Figure 1h and i, the expression level of those ER stress proteins including GRP78, Calnexin, phosphorylated eIF2α and eIF2α (15) as well as spliced XBP1 mRNA (15) was not altered (Figure 1i), suggesting that non-targeting siRNA did not trigger the canonical ER stress pathways. Thus, non-targeting shRNA/siRNA may pose a unique stress that selectively upregulates NPGPx expression.

Persistent expression of non-targeting shRNA/siRNA retards cell growth with a prolonged G1 phase

It was reported that off-targeting shRNA/siRNA may cause the exhaustion of RISC to generate cellular stress resulted in growth retardation and cell death (10). To test whether persistent expression of non-targeting shRNA also inhibits cell growth, we compared the proliferation profiles of a pair of MEFs with NPGPx proficiency or deficiency (Figure 2a). Expression of non-targeting shRNA in NPGPx-proficient MEFs retarded their growth, while no obvious inhibition was found in NPGPx-deficient MEFs (Figure 2b). Consistently, FACS analysis of cell cycle profiles revealed that higher percentage of normal cells (MEFs and WI38 cells) with non-targeting shRNA/siRNA prolonged G1 phase compared with those without shRNA (Figure 2c and d). These results suggest that expression of non-targeting siRNA generates a stress, which retards cell growth and prolongs G1 phase.

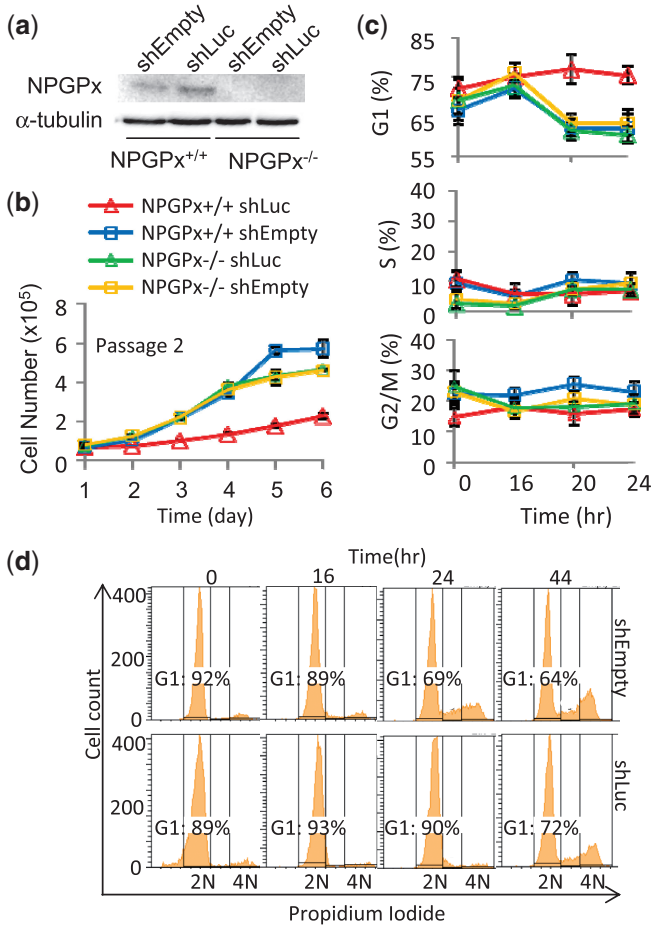

Figure 2. Cells suffering from non-targeting siRNA stress grew slowly with prolonged G1 phase. (**a**) Western blot analysis using MEFs (WT or NPGPx$^{-/-}$ MEFs) transduced with shLuc or control vector (shEmpty). (**b**) Cell growth assay. MEFs (WT or NPGPx$^{-/-}$ MEFs) at early passages transduced with shLuc or control vector (shEmpty) were seeded by equal amount (1×10^5 cell/dish) in 6 cm dishes, and cell numbers were counted every day. (**c**) Cell cycle analysis by FACS was performed at 0, 16, 20 or 24 h after cells were released from starvation. The percentages of cells in G1, S or G2/M phase were shown individually by plot. (**d**) Cell cycle profiles of WI38 cells transduced with shLuc or control vector (shEmpty). WI38 cells were synchronized with serum starvation, and the cell cycle analysis was performed at 0, 16, 24, 44 h after cells released from starvation. The percentage of cells in G1 phase was shown on each plot. These experiments have been repeated three times with similar results.

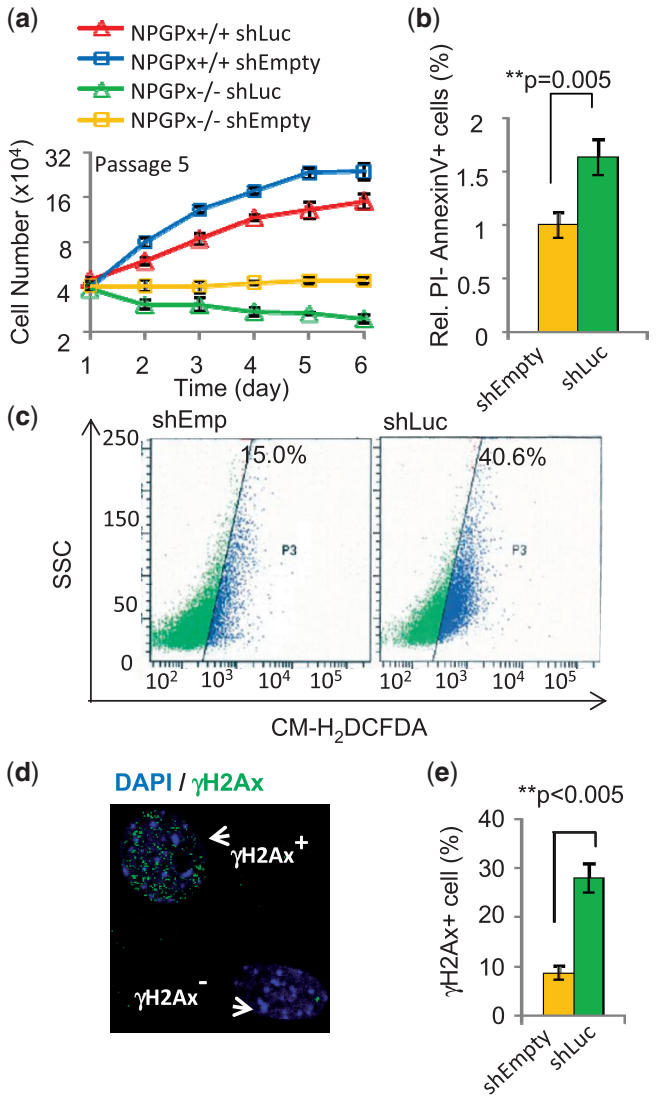

Figure 3. Persistent exposure to non-targeting siRNA stress led to ROS production, DNA damage and apoptosis in NPGPx$^{-/-}$ MEFs. (**a**) Cell growth patterns of MEFs at passage 5. (**b**) Annexin V staining. NPGPx$^{-/-}$ MEFs at the fourth day from (a) were stained with Annexin V and PI. Percentage of the apoptotic (Annexin V+PI−) cell was illustrated. $^{**}P = 0.005$. (**c**) Endogenous ROS measurement. NPGPx$^{-/-}$ MEFs [same as in (b)] were stained with CM-H_2DCFDA (29) which converted into a green florescence when encounters intracellular ROS, and analyzed by FACS. (**d**) A representative γH2Ax IF staining with green florescence of NPGPx$^{-/-}$ MEFs [same with (b)]. Blue: DAPI. (**e**). The percentage of γH2Ax positive staining cells from (d). These experiments have been repeated three times.

Expression of non-targeting shRNA/siRNA in NPGPx$^{-/-}$ cells leads to ROS production, genome damage and cell death

NPGPx$^{-/-}$ MEFs appeared to be unresponsive transiently to non-targeting siRNA-induced growth retardation (Figure 2b). To investigate the consequence of the insensitivity to this stress, we therefore compared the growth rate between wild-type and NPGPx$^{-/-}$ MEFs at late passage (passage 5) under persistent non-targeting shRNA/siRNA stress. Wild-type MEF grew slower at late passage, while NPGPx$^{-/-}$ cell numbers reduced steadily (Figure 3a). Using annexin V staining assay, those cells were undergoing apoptosis (Figure 3b). Moreover, ROS level was highly elevated in non-targeting shRNA/siRNA stressed NPGPx$^{-/-}$ MEFs when compared with the unstressed MEFs (Figure 3c). Consistently, the stressed NPGPx$^{-/-}$ MEFs had more γH2AX foci compared with the unstressed cells (Figure 3d and e). These results suggest that there were more damaged DNA in non-targeting siRNA stressed cells than unstressed cells. Thus, persistent non-targeting shRNA/siRNA stress can lead to elevated ROS, genome damage and apoptosis in NPGPx$^{-/-}$ cells, indicating the importance of NPGPx for cells to mediate this stress.

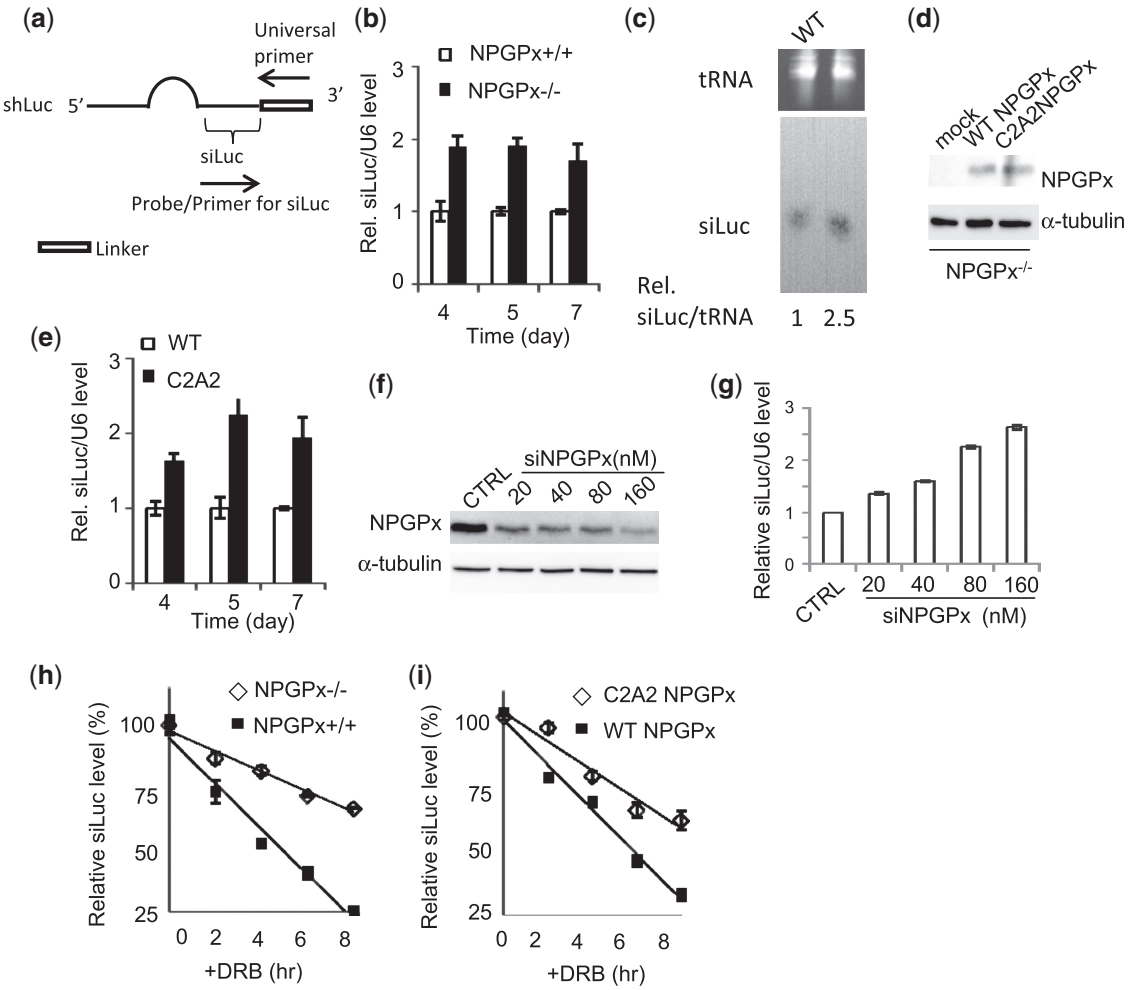

Figure 4. NPGPx was required for releasing non-targeting siRNA stress. (**a**) Schematic of primers designed for siRNA detection. (**b**) Steady amount of siLuc in MEFs transduced with shLuc. MEFs transduced with shLuc were used for measuring siLuc/U6 ratio by RT–qPCR at 4, 5, 7 days after shLuc-lentivirus infection. siLuc RNA accumulation was observed in NPGPx$^{-/-}$ MEFs. (**c**) Northern blot analysis of RNA from WT or NPGPx$^{-/-}$ MEFs transduced with shLuc probed with biotinylated-RNA against siLuc. tRNA was used as a loading control. The relative siLuc/tRNA ratio (Rel. siLuc/tRNA) was shown. (**d**) Western blot analysis of NPGPx protein using NPGPx$^{-/-}$ MEFs restored with WT or mutant NPGPx (C2A2-NPGPx). α-Tubulin served as an internal control. Mock: MEFs without retroviral transduction. (**e**) Steady amount of siLuc in MEFs transduced with shLuc. MEFs transduced with shLuc were used for measuring siLuc/U6 ratio by RT–qPCR as descrived in (b). siLuc accumulation was found in C2A2-NPGPx restored MEFs compared with control MEFs (WT or WT-NPGPx restored MEFs). (**f**) NPGPx protein expression level of MEFs transfected with 160 nM control non-targeting siRNA (CTRL) or siNPGPx. (**g**) siLuc RNA level in NPGPx-depleted MEFs. WT MEFs expressing shLuc were transfected with increasing amount of NPGPx siRNA. The ratios of cellular siLuc and U6 RNA were measured by RT–qPCR. CTRL: MEFs cells transfected with 160 nM non-targeting siRNA. (**h** and **i**) Stability of siLuc measured by RT–qPCR using DRB-treated MEFs. Equal amount of reverse-transcribed RNA was used in the RT–qPCR analysis. Relative siLuc level (relative to 0 h) was shown. The kinetic plot indicated that the siLuc had a slower turnover rate in NPGPx$^{-/-}$ MEFs (h) and C2A2-restored MEFs (i) when compared with control MEFs. Each experiment has been repeated more than three times, and the representative data from one of these experiments were shown.

NPGPx is required for eliminating non-targeting siRNA

It is well documented that stress-induced proteins usually are functional in releasing the stress. For example, GRP78 expression was induced by ER stress to release the ER stress (15). As described above, NPGPx was induced by siRNA stress, and therefore it is likely that NPGPx contributes to eliminate non-targeting siRNA accumulation. In order to measure mature siLuc RNA level, we first reversely transcribed siRNAs as previously described (16) and then used a primer (primer for siLuc, Figure 4a) that recognized the sense strand of shLuc (i.e. siLuc) for qPCR analysis. Since this primer sequence was also complimentary to shLuc, siLuc and shLuc were all amplified by using this set of primer in qPCR analysis. Therefore, another primer targeting to the stem–loop region of shLuc was designed to distinguish the precursor shLuc from siLuc. When shLuc and siLuc RNA were measured by qPCR, the shLuc RNA level was at least 200-fold lower than siLuc (data not shown). Thus, the shRNA contributed very little to the overall siRNA concentration. Based on the observation, we measured the siLuc concentration relative to U6 RNA of WT and NPGPx$^{-/-}$ MEFs, and found that NPGPx^{--} MEFs contained about 2-fold higher siLuc than that of in WT cells (Figure 4b). Similarly, using direct RNA blotting, NPGPx$^{-/-}$ MEFs also contained 2.5-folds higher siLuc RNA than WT cells

(Figure 4c). To confirm whether NPGPx is responsible for the difference, we generated NPGPx$^{-/-}$ MEFs expressing either WT NPGPx or C2A2 mutant through retroviral-mediated gene transfer (Figure 4d and e). Since two cysteines, Cys57 and Cys86, were essential for NPGPx biochemical activity, changing these two residues into alanine as C2A2 mutant completely inactivated its function (Wei *et al.*, manuscript in preparation). By comparing these two MEFs, we found that C2A2 expressing NPGPx$^{-/-}$ cells contained about 2.5-folds siLuc higher than that of in WT NPGPx-expressing cells (Figure 4e), suggesting that active NPGPx was required for reducing non-targeting siRNA. Similarly, depletion of NPGPx by siRNA in human fibroblast cells increased the siLuc level (Figure 4f and Figure 4g). Next, to test whether the high level of siLuc in NPGPx-deficient cells may result from slow turnover, we used 5,6-dichloro-1-β-D-ribofuranosylbenzimidazole(DRB), which inhibits RNA Pol II phosphorylation and blocks transcription (17), to treat cells and measured the siLuc turnover kinetics (Figure 4h and i). As shown in Figure 4h, siLuc was degraded faster in WT MEFs compared with NPGPx-deficient cells. Consistently, the degradation rate of siLuc in WT-expressing cells was faster than C2A2 mutant-expressing cells (Figure 4i). These results support the notion that NPGPx is essential for reducing the accumulation of non-targeting siRNA.

XRN2, an NPGPx-interacting exoribonuclease, plays a role in releasing non-targeting siRNA

NPGPx does not have the required RNAse activity for the removal of the accumulated non-targeting siRNA. It is likely that NPGPx may modulate protein/enzymes for this purpose. To search for such potential enzymes, we incubated cell lysate with NPGPx-immobolized beads and eluted the bound proteins by cleavage with TEV protease for mass spectrometry (Wei *et al.*, unpublished data). One of those proteins, which covalently bound to NPGPx, was the 5′–3′ exoribonuclease, XRN2, which participates in siRNA/miRNA metabolism (18). To test whether XRN2 plays a direct role in removing non-targeting siRNA, we depleted XRN2 from WI38 fibroblasts by two different shRNAs and found that the cells accumulated the non-targeting siRNA (Figure 5a and b). To test whether NPGPx and XRN2 are functional in the same process, we compared the amount of the accumulated non-targeting siLuc between wild-type and NPGPx$^{-/-}$ MEFs upon depletion of XRN2. In wild-type MEF, non-target siRNA was increased upon the depletion of XRN2, while in NPGPx$^{-/-}$ MEFs, which had a higher basal level, the accumulation of non-targeting siRNA was not further increased (Figure 5c and d). Consistently, NPGPx$^{-/-}$ MEF expressing WT NPGPx accumulated high siLuc upon depletion of XRN2 (Figure 5f, open bar), while cells expressing C2A2 mutant the siLuc level was not affected by XRN2 silencing (Figure 5f, filled bar). Taken together, these results suggest that NPGPx and XRN2 work together in the same pathway in removing non-targeting siRNA.

NPGPx interacts with XRN2

To further demonstrate that these two proteins directly work together, we then tested whether these two proteins interact *in vivo*. As shown in Figure 6a,

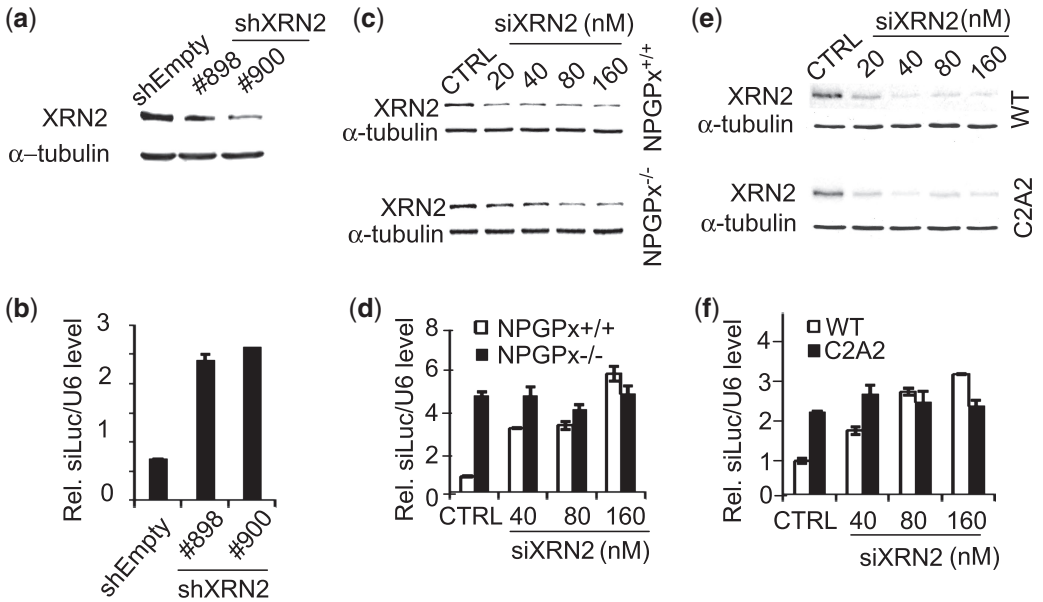

Figure 5. NPGPx and XRN2 were associated for releasing non-targeting siRNA. (**a**) Western blot analysis of XRN2 protein expression in shLuc-expressing WI38 cells infected with lentiviruses carrying with XRN2 shRNAs (two clones as indicated) or shEmpty as control. (**b**) RT–qPCR analysis of relative siLuc expression level normalized to U6 in XRN2-depleted WI38 cells. (**c** and **e**) Western blot analysis of XRN2 from WT, NPGPx$^{-/-}$ MEFs (c) or NPGPx$^{-/-}$ MEFs expressing WT or C2A2 mutant (e). MEFs were transfected with either 160 nM non-targeting siRNA (CTRL) or XRN2 siRNA (siXRN2), and analyzed XRN2 protein level by western blot. α-Tubulin serves as an internal control. (**d** and **f**) RT–qPCR analysis of relative siLuc expression level in XRN2-depleted MEFs. siLuc RNA level was normalized with U6 RNA level. This experiment has been repeated twice.

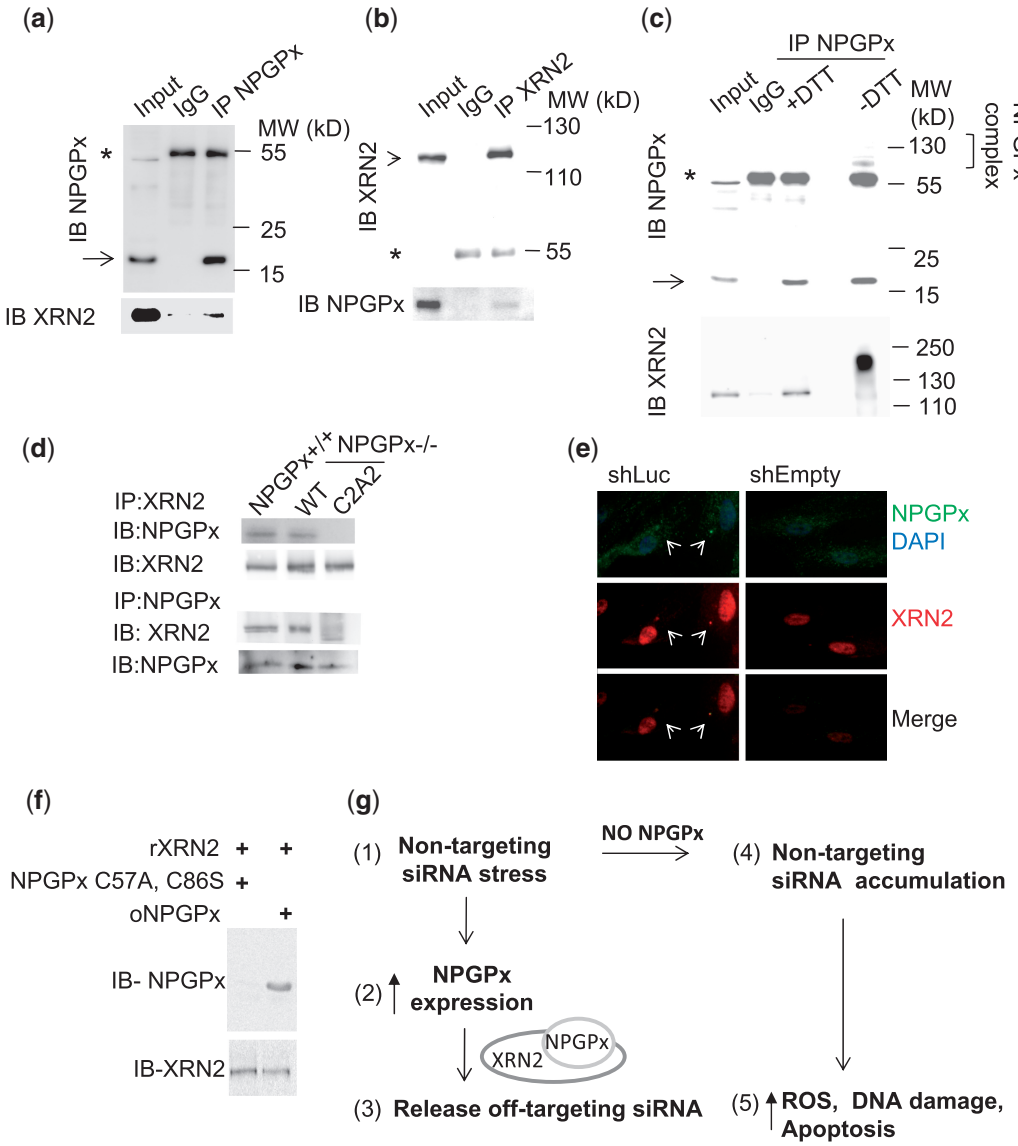

Figure 6. NPGPx and XRN2 interacted through covalent bonding. (**a** and **b**) NPGPx was reciprocally coimmunoprecited with XRN2. Cell lysates prepared from WI38 cells transduced with shLuc were used in this experiment. Asterisk: heavy chain; arrow: NPGPx. (**c**) NPGPx and XRN2 were covalently associated. Immunocomplexes of NPGPx and XRN2 were analyzed by SDS–PAGE before adding or without reducing agent (+DTT or −DTT). NPGPx and XRN2 were then blotted as indicated. (**d**) Coimmunoprecipitation analysis of XRN2 with WT NPGPx and C2A2 mutant in shLuc-expressing MEFs. Cell lysates prepared from NPGPx −/− MEFs expressing WT or C2A2 mutant were used. Immunoprecipitated complexes were separated by SDS–PAGE and probed by XRN2- or NPGPx-specific antibodies. (**e**) Immunofluorescence staining of WI38 cells transduced with shLuc or control vector (shEmpty). Green: NPGPx; red: XRN2; blue: DAPI. (**f**) NPGPx and XRN2 interacted directly *in vitro*. Purified XRN2 (rXRN2) were immobilized on nickel column, and incubated with purified NPGPx (oxidized form, oNPGPx) or C2AS mutant (C57AC86S). NPGPx and XRN2 complex were eluted by imidazole and analyzed by western blot. These experiments have been repeated three times. (**g**) Model for NPGPx responding to non-targeting siRNA stress. When cells experienced non-targeting siRNA stress, NPGPx expression was induced (1) and in turn activated XRN2 (2) to release/reduce non-targeting siRNA (3). In contrast, cells without NPGPx will accumulate non-targeting siRNA stress (4) and result in DNA damage, elevated ROS and apoptosis (5).

immunoprecipitation (IP) of NPGPx brought down XRN2. Reciprocally, NPGPx could be detected in the immunoprecipitated XRN2 complex (Figure 6b). It was noteworthy that NPGPx-XRN2 complex was held through disulfide bond, because the immunoprecipitated complex migrated in a much higher molecular weight in SDS–PAGE without treatment with reducing agent (Figure 6c). To further verify that the disulfide bonding was critical for the interaction, we used NPGPx$^{-/-}$ cells expressing WT or C2A2-mutant for co-immunoprecipitation experiment, and found that XRN2 associated with WT but not C2A2 mutant (Figure 6d). XRN2 is a nuclear protein (19). A small portion of XRN2 apparently was translocated to cytoplasm when cells suffered from non-targeting siRNA stress (Figure 6e). The cytosolic XRN2 appeared to be colocalized with NPGPx in specific foci (Figure 6e). Finally, to test whether these two proteins interact directly, we performed *in vitro* binding assay using purified proteins of WT NPGPx, C2AS-mutant and

XRN2. It was noted that C2AS mutant had a better solubility than C2A2. His-XRN2 was first immobilized on nickel beads and then incubated with WT or C2AS mutant separately. After washing with 8M Urea, the covalently bound NPGPx-XRN2 was eluted and detected by western blot. As shown in Figure 6g, XRN2 directly bound to WT NPGPx, but not C2AS mutant. These data suggest that NPGPx and XRN2 interact through covalent bonding when encountered with non-targeting siRNA stress, and these covalent interaction required Cys57 and Cys86 of NPGPx.

DISCUSSION

In this communication, we found that non-targeting siRNA is a stress that induces NPGPx expression, which co-operates with XRN2 to eliminate the accumulated non-targeting siRNAs (Figure 6g). Under non-targeting siRNA stress, NPGPx-proficient cells exhibited a slower growth rate with a slightly prolonged G1 phase, while NPGPx-deficient cells elevated endogenous ROS production and underwent apoptosis. Non-targeting siRNA apparently is a stress. Since control siRNAs are frequently used in research laboratories and in clinical experiments, the unintended consequence from the usage of non-targeting siRNA may cause interference. Precaution must be taken to avoid this side effect. One may use a low dose of scramble siRNA instead of non-targeting siRNA (for example, <20 nM per experiment). Based on our findings, we recommend that each control siRNA be tested for causing the non-targeting siRNA effect by screening NPGPx expression.

In addition to NPGPx, expressions of other genes induced by non-targeting siRNA have been reported (20) although their precise functions remain to be addressed. Translation of mRNA mainly takes place on ER membrane. It was thought that the constitutively activated siRISC due to overexpressing siRNA might cause ER stress. However, neither ER chaperons (GRP78 or Calnexin) nor ER-stress responding factors (eIF2α and XBP-1) were affected upon non-target siRNA (Figure 1, shEmpty). Similarly, NPGPx was not induced by neither virus infection (Figure 1) nor exogenouse viral RNA analog poly(dI:dC) transfection (data not shown). These results suggest that non-targeting siRNA expression causes a unique stress response that does not involve the canonical ER-stress or viral infection-induced signal pathway.

Cells suffering from non-targeting siRNA stress retarded growth and prolonged G1 phase (Figure 2). This phenotype can be explained as cells required time to resolve the non-targeting siRNA stress before progressing to S phase. Intriguingly, such observed phenotype was not seen in early passaged NPGPx$^{-/-}$ MEFs (Figure 2). However, NPGPx$^{-/-}$ MEFs with continuous non-targeting siRNA stress resulted in the elevation of ROS, DNA damage and cell death (Figure 3). Accumulated non-targeting siRNAs in NPGPx$^{-/-}$ cells may impair the turnover of the available RISC and in turn elevate ROS. Another possibility is that the accumulated siRNA may ultimately be recognized as foreign viral RNA and trigger antiviral responses as reported of human T-cell leukemia virus type 1 (HTLV-1) (21) and hepatitis C virus (HCV) (22), and activate interferon signal pathway (20) to antagonize infection-like RNA stress. Thus, induction of NPGPx expression may be a self-preservation mechanism to protect cells from damages caused by non-targeting siRNA. Similar observation was also reported in p53-deficient cells, which were not arrested in G1 under ionizing radiation (IR) (23), while p53$^{-/-}$ mice developed cancer by the age of 3-month (24). Thus, induction of NPGPx expression is critical for cells to resolve the non-targeting siRNA stress.

It remains unclear how cells sense the non-targeting siRNA stress to activate NPGPx. Since the non-targeting siRNA stress is distinct from the current known ER stress and interferon-induced stress response pathways, a novel signal pathway that transmits the stress signal from the accumulated siRISC complex to responders must exist. Our preliminary data suggested that the NPGPx promoter was transactivated by nucleolin (Wei *et al.*, manuscript in preparation). It is likely that the stress signal will pass this message to nucleolin and/or other factors to activate NPGPx expression. Obviously, elucidating this novel signal pathway will be both challenging and interesting.

NPGPx belongs to the glutathione peroxidase (GPX) family based on its primary sequence alignment; however, it did not have glutathione peroxidase activity (Lee *et al.*, unpublished data). NPGPx may use its two residues, Cys57 and Cys86, to activate other protein or enzyme via disulfide shuttling. The yeast GPX-3 has been shown to behave in a manner similar to NPGPx as described above (25). Recently, a nuclear 5′–3′ exoribonuclease, XRN2, was identified to be responsible for degrading a subset of miRNA in *C. elegans* (26). Its homolog XRN1 was found to promote mature mir-382 and mir-378 decay in HEK293 cells (27). Consistent with our observation described here, NPGPx bound to and positively modulated XRN2 in releasing the accumulated non-targeting siRNAs. Interestingly, when we aligned the amino acid sequences of XRN2, we found that most of the 16 cysteine residues are conserved in yeast and human, suggesting the importance of these cysteines for XRN2 function. Since XRN2 covalently bound to NPGPx *in vivo* and *in vitro* (Figure 6), it is likely that NPGPx may facilitate the disulfide bond formation of XRN2 to activate its enzymatic activity. Consistent to this scenario, C2A2 mutant was not able to cooperate with XRN2 in responding to non-targeting siRNA stress. However, the detailed biochemical mechanism of this activation warrants further investigation.

It was reported that Ago2 carrying with sense strand miRNA/siRNA, together with the targeting mRNA, translocates from nucleus to cytosolic P-body (28). The translocation of Ago2-miRNA-targeting mRNA was aimed to degrade the mRNA there. Interestingly, we observed that NPGPx and XRN2 also translocalized to the distinct cytosolic foci under non-targeting siRNA stress (Figure 6e). Thus, it is likely that non-targeting

siRNA would go through a similar degradation pathway along with Ago2 and XRN2 in P-body, because we also observed that Ago2 and XRN2 were colocalized in the cytosolic foci in our preliminary result. Nevertheless, how NPGPx translocates to these distinct cytosolic foci and what kind of post-translational modification occurs to NPGPx warrant further investigation.

ACKNOWLEDGEMENT

We thank Dr Wendy Hwang-Verslues for critical proof-reading of the manuscript and Ms Meng-Han Wang for her kind assistance through this study.

FUNDING

Funding for open access charge: Academia Sinica, Taiwan and Philip Morris Foundation, USA.

Conflict of interest statement. According to UCI policy, W.-H.L. declares that he serves as a board member of the biotech company, GeneTex, and has equality interest. This arrangement has been reviewed and approved by UCI COI committee.

REFERENCES

1. van der Krol,A.R., Mur,L.A., Beld,M., Mol,J.N. and Stuitje,A.R. (1990) Flavonoid genes in petunia: addition of a limited number of gene copies may lead to a suppression of gene expression. *Plant Cell*, **2**, 291–299.
2. Napoli,C., Lemieux,C. and Jorgensen,R. (1990) Introduction of a chimeric chalcone synthase gene into petunia results in reversible co-suppression of homologous genes in trans. *Plant Cell*, **2**, 279–289.
3. Fire,A., Xu,S., Montgomery,M.K., Kostas,S.A., Driver,S.E. and Mello,C.C. (1998) Potent and specific genetic interference by double-stranded RNA in Caenorhabditis elegans. *Nature*, **391**, 806–811.
4. Zamore,P.D., Tuschl,T., Sharp,P.A. and Bartel,D.P. (2000) RNAi: double-stranded RNA directs the ATP-dependent cleavage of mRNA at 21 to 23 nucleotide intervals. *Cell*, **101**, 25–33.
5. Robb,G.B. and Rana,T.M. (2007) RNA helicase A interacts with RISC in human cells and functions in RISC loading. *Mol. Cell*, **26**, 523–537.
6. Elbashir,S.M., Lendeckel,W. and Tuschl,T. (2001) RNA interference is mediated by 21- and 22-nucleotide RNAs. *Genes Dev.*, **15**, 188–200.
7. Liu,J. (2008) Control of protein synthesis and mRNA degradation by microRNAs. *Curr. Opin. Cell Biol.*, **20**, 214–221.
8. Clark,P.R., Pober,J.S. and Kluger,M.S. (2008) Knockdown of TNFR1 by the sense strand of an ICAM-1 siRNA: dissection of an off-target effect. *Nucleic Acids Res.*, **36**, 1081–1097.
9. Birmingham,A., Anderson,E.M., Reynolds,A., Ilsley-Tyree,D., Leake,D., Fedorov,Y., Baskerville,S., Maksimova,E., Robinson,K., Karpilow,J. *et al.* (2006) 3′ UTR seed matches, but not overall identity, are associated with RNAi off-targets. *Nat. Methods*, **3**, 199–204.
10. Fedorov,Y., Anderson,E.M., Birmingham,A., Reynolds,A., Karpilow,J., Robinson,K., Leake,D., Marshall,W.S. and Khvorova,A. (2006) Off-target effects by siRNA can induce toxic phenotype. *RNA*, **12**, 1188–1196.
11. Chen,C.F., Chen,Y., Dai,K., Chen,P.L., Riley,D.J. and Lee,W.H. (1996) A new member of the hsp90 family of molecular chaperones interacts with the retinoblastoma protein during mitosis and after heat shock. *Mol. Cell. Biol.*, **16**, 4691–4699.
12. Liu,C.G., Calin,G.A., Meloon,B., Gamliel,N., Sevignani,C., Ferracin,M., Dumitru,C.D., Shimizu,M., Zupo,S., Dono,M. *et al.* (2004) An oligonucleotide microchip for genome-wide microRNA profiling in human and mouse tissues. *Proc. Natl Acad. Sci. USA*, **101**, 9740–9744.
13. Stols,L., Gu,M., Dieckman,L., Raffen,R., Collart,F.R. and Donnelly,M.I. (2002) A new vector for high-throughput, ligation-independent cloning encoding a tobacco etch virus protease cleavage site. *Protein Exp. Purif.*, **25**, 8–15.
14. Zheng,L., Pan,H., Li,S., Flesken-Nikitin,A., Chen,P.L., Boyer,T.G. and Lee,W.H. (2000) Sequence-specific transcriptional corepressor function for BRCA1 through a novel zinc finger protein, ZBRK1. *Mol. Cell*, **6**, 757–768.
15. Ron,D. and Walter,P. (2007) Signal integration in the endoplasmic reticulum unfolded protein response. *Nat. Rev. Mol. Cell Biol.*, **8**, 519–529.
16. Bemis,L.T., Chen,R., Amato,C.M., Classen,E.H., Robinson,S.E., Coffey,D.G., Erickson,P.F., Shellman,Y.G. and Robinson,W.A. (2008) MicroRNA-137 targets microphthalmia-associated transcription factor in melanoma cell lines. *Cancer Res.*, **68**, 1362–1368.
17. Marshall,N.F., Peng,J., Xie,Z. and Price,D.H. (1996) Control of RNA polymerase II elongation potential by a novel carboxyl-terminal domain kinase. *J. Biol. Chem.*, **271**, 27176–27183.
18. Gy,I., Gasciolli,V., Lauressergues,D., Morel,J.B., Gombert,J., Proux,F., Proux,C., Vaucheret,H. and Mallory,A.C. (2007) Arabidopsis FIERY1, XRN2, and XRN3 are endogenous RNA silencing suppressors. *Plant Cell*, **19**, 3451–3461.
19. Wang,M. and Pestov,D.G. (2010) 5′-end surveillance by Xrn2 acts as a shared mechanism for mammalian pre-rRNA maturation and decay. *Nucleic Acids Res.*, **39**, 1811–1822.
20. Persengiev,S.P., Zhu,X. and Green,M.R. (2004) Nonspecific, concentration-dependent stimulation and repression of mammalian gene expression by small interfering RNAs (siRNAs). *RNA*, **10**, 12–18.
21. Kinjo,T., Ham-Terhune,J., Peloponese,J.M. Jr and Jeang,K.T. (2010) Induction of reactive oxygen species by human T-cell leukemia virus type 1 tax correlates with DNA damage and expression of cellular senescence marker. *J. Virol.*, **84**, 5431–5437.
22. Pal,S., Polyak,S.J., Bano,N., Qiu,W.C., Carithers,R.L., Shuhart,M., Gretch,D.R. and Das,A. (2010) Hepatitis C virus induces oxidative stress, DNA damage and modulates the DNA repair enzyme NEIL1. *J. Gastroenterol. Hepatol.*, **25**, 627–634.
23. Lowe,S.W., Schmitt,E.M., Smith,S.W., Osborne,B.A. and Jacks,T. (1993) p53 is required for radiation-induced apoptosis in mouse thymocytes. *Nature*, **362**, 847–849.
24. Donehower,L.A., Harvey,M., Slagle,B.L., McArthur,M.J., Montgomery,C.A. Jr, Butel,J.S. and Bradley,A. (1992) Mice deficient for p53 are developmentally normal but susceptible to spontaneous tumours. *Nature*, **356**, 215–221.
25. Delaunay,A., Pflieger,D., Barrault,M.B., Vinh,J. and Toledano,M.B. (2002) A thiol peroxidase is an H2O2 receptor and redox-transducer in gene activation. *Cell*, **111**, 471–481.
26. Chatterjee,S. and Grosshans,H. (2009) Active turnover modulates mature microRNA activity in Caenorhabditis elegans. *Nature*, **461**, 546–549.
27. Bail,S., Swerdel,M., Liu,H., Jiao,X., Goff,L.A., Hart,R.P. and Kiledjian,M. (2010) Differential regulation of microRNA stability. *RNA*, **16**, 1032–1039.
28. Liu,J.D., Valencia-Sanchez,M.A., Hannon,G.J. and Parker,R. (2005) MicroRNA-dependent localization of targeted mRNAs to mammalian P-bodies. *Nat. Cell Biol.*, **7**, 719–723.
29. O'Donovan,P., Perrett,C.M., Zhang,X., Montaner,B., Xu,Y.Z., Harwood,C.A., McGregor,J.M., Walker,S.L., Hanaoka,F. and Karran,P. (2005) Azathioprine and UVA light generate mutagenic oxidative DNA damage. *Science*, **309**, 1871–1874.